ACS OMEGA

Open Access

http://pubs.acs.org/journal/acsodf

Article

Cu(II)-Catalyzed Synthesis of Pyrazolo[3,4-*b*]pyridine Derivatives and Their Potential Antibacterial and Cytotoxic Activities with Molecular Docking, DFT Calculation, and SwissADME Analysis

Velmurugan Loganathan, Anis Ahamed, Idhayadhulla Akbar,* Desta Galcha Gerbu, Hissah Abdulrahman Alodaini, and Aseer Manilal

Cite This: *ACS Omega* 2025, 10, 1643−1656

Read Online

ACCESS | Metrics & More | Article Recommendations | Supporting Information

ABSTRACT: The present work focuses on a newly synthesized pyrazolo[3,4-*b*]pyridine prepared by formal [3 + 3] cycloaddition using copper(II) acetylacetonate as the catalyst; efficient and effective mild reactions with high yields were obtained using this method. The synthesized compounds were identified by FT-IR, ^{1}H and ^{13}C NMR, and mass spectra (*m*/*z*) analyses. The compounds (**2a**−**l**) were screened for several in vitro and in silico activities. Compound **2g** showed impressive inhibitory activities against methicillin-resistant *Staphylococcus aureus* (MIC: 2 μg/mL), vancomycin-resistant Enterococci (MIC: 8 μg/mL), piperacillin-resistant *Pseudomonas aeruginosa*, and extended-spectrum beta-lactamase-producing *Escherichia coli* (MIC: 4 μg/mL) compared to the positive control, ciprofloxacin. Compared to standard doxorubicin, compound **2g** had a higher efficacy against the HepG2 cancer cell line, with a GI_{50} value of 0.01 μM. The highly active compound **2g** was investigated for in silico molecular docking, density functional theory calculations (DFT), and SwissADME physicochemical properties. Compound **2g** had a higher docking score compared with standard (−8.5 vs −7.3 and −10.0 vs −8.4 kcal/mol). In compound **2g**, the energy gap was 0.17 eV, as determined by using DFT calculations. The physicochemical properties of all compounds were investigated by using SwissADME. Overall, compound **2g** exhibited promising antibacterial and cytotoxic activities.

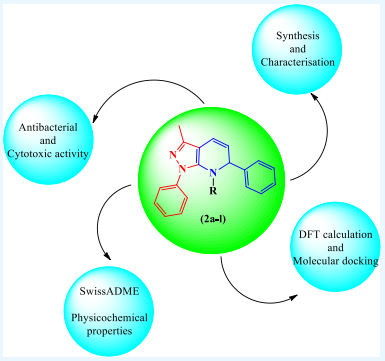

INTRODUCTION

The broad range of biological and pharmacological uses of nitrogen-containing heterocyclic molecules has sparked significant interest in their production.[1,2] The features of all heterocyclic skeletons are united when two or more distinct heterocyclic moieties are present in a single molecule, which may eventually improve the pharmacological or biological activity. As a result of their diverse applications, the synthesis of new polycyclic heterocycles through the combination of various structural motifs has recently attracted a great deal of attention.[3,4] Several pyrazole derivatives are known to exhibit diverse biological and pharmacological activities, including antibacterial,[5] pesticide,[6] fungicidal,[7] antihypertensive,[8] anticancer,[9] and antimicrobial properties.[10] Heterocyclic frameworks, including pyrazole, have a multitude of applications, owing to their adaptability to bioactive substances. The pyrazole [3,4-*b*] pyridine-fused system has been reported for its FGFR kinase inhibitory, antimicrobial, anticancer, larvicidal, and cytotoxic activities.[11−17] Consequently, the pyrazole-pyridine connection and essential ingredients of many bioactive compounds have gained greater attention in recent years.[18,19] Pyrazolo[3,4-*b*]pyridine exists in various drug molecules such as cartazolates, etazolates, tracazolate, and riociguat, which are used for hypertension,[20−22] as shown in Figure 1.

To produce pyrazolo[3,4-*b*]pyridine analogues embellished with relevant pharmacophores concurrently, a number of pyrazolo[3,4-*b*]pyridine cores are readily synthesized using innovative methods based on different substrates. The methods used to synthesize pyrazolo[3,4-*b*] pyridine, which utilizes aromatic aldehydes, 5-amino pyrazole, and active methylene compounds or 1,3-diketones, have been previously reported. Furthermore, various innovative approaches utilizing novel substances have been developed, eventually leading to the synthesis of pyrazolo[3,4-*b*]pyridine core compounds. Pyrazolo[3,4-*b*]pyridine was synthesized by using various catalysts such as MgO/HAp,[23] pTSA,[24] acetonitrile by H_2O_2-mediated oxidation,[25] copper(II)oxide nanoparticles,[26] aluminum oxide,[27] Fe_3O_4@MIL-101(Cr)−$N(CH_2PO_3)_2$,[28] and UiO-66-NH_2/TCT/2-amino-Py@$Cu(OAc)_2$, and silica sulfuric acid.[29,30] In the synthesis of heterocyclic compounds, multicomponent reactions are crucial because they allow for

Received: October 19, 2024
Revised: December 17, 2024
Accepted: December 19, 2024
Published: December 25, 2024

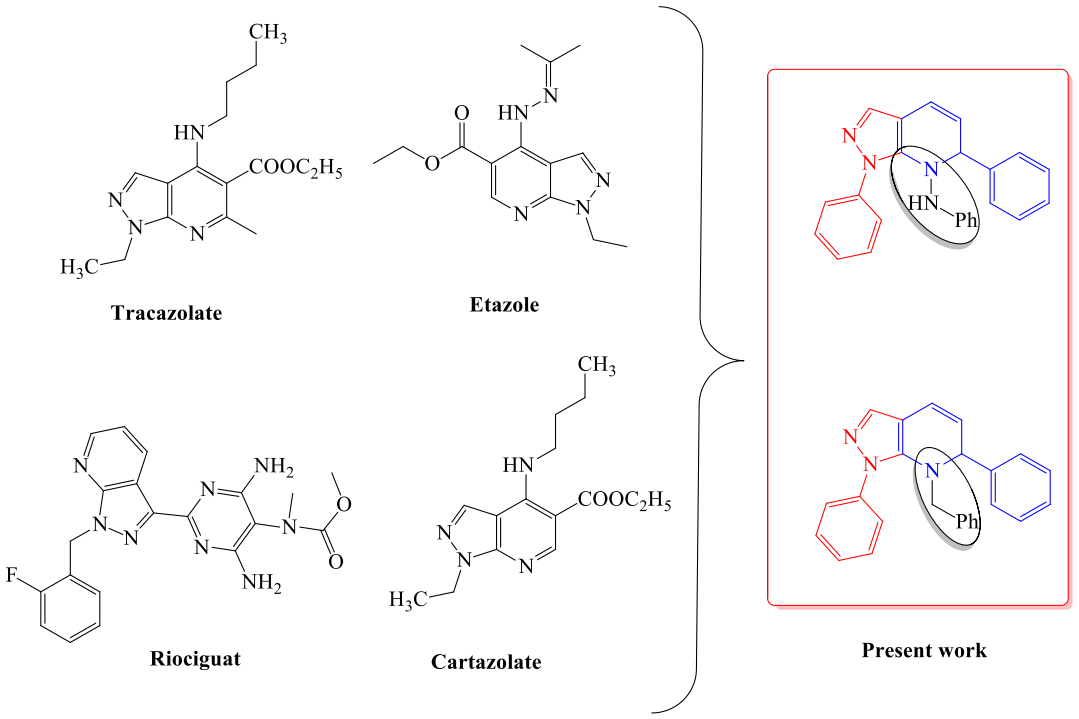

Figure 1. Bioactive 1*H*-pyrazolo [3,4-*b*]pyridine derivatives.

numerous bond-making or bond-breaking reactions in an economically and ecologically beneficial one-pot procedure.[31−33]

The antibacterial properties of a molecule are mainly determined by its ability to either directly kill bacteria or inhibit their growth without causing significant harm to the surrounding tissues.[34,35] Cytotoxicity refers to the capacity of a molecule to affect cell growth and proliferation.[36] The antimicrobial and anticancer properties of natural compounds present a promising therapeutic opportunity. These compounds can selectively target and eliminate cancer cells while also reducing the risk of opportunistic infections in immunocompromised cancer patients, making them a viable treatment option.[37] Previous studies have documented the antibacterial and cytotoxic activities of pyrazolo[3,4-*b*]pyridine derivatives.[38−41]

According to a literature search, no studies have been conducted on the copper(II) acetylacetonate catalyst used for the synthesis of pyrazolo[3,4-*b*]pyridine and its antibacterial activity. The current research focuses on the comparison of various copper(II) catalysts, emphasizing ring-closure strategies and synthetic diversity for the cyclization of [3 + 3] cycloaddition reactions, as well as their antibacterial and cytotoxic properties and in silico molecular docking, density functional theory (DFT) calculations, and physicochemical properties.

EXPERIMENTAL SECTION

Materials and Methods. All analytical-grade chemicals were purchased from Sigma-Aldrich. Melting points were observed in the open capillary tubes. The FT-IR data range 4000−400 cm^{-1} was recorded using a Thermo Scientific Nicolet iS5 (KBR Windows Spectrometer) instrument. Using DMSO-d_6 as the solvent, NMR was conducted at 300 and 75 MHz on a Bruker spectrometer. The elements (C, H, N, and S) were detected using an elemental analyzer (Varian EL III).

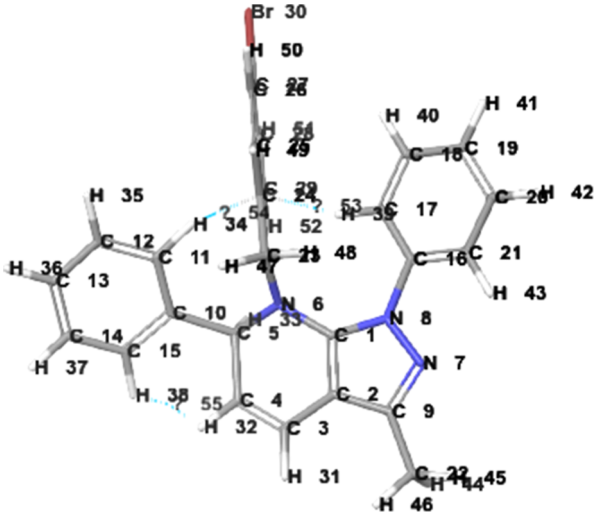

Figure 2. Atom numbering of compound **2g**.

Mass spectra were obtained using a PerkinElmer GCMS model Clarus 690-SQ8MS (EI) instrument.

General Procedures for Compound 1a. The compound 3-methyl-1-phenyl-1*H*-pyrazol-5(4*H*)-one (0.01 mol, 1.7408 g) was combined with hydrazine and ground in a mortar and pestle for 15 min at room temperature. After filtering and washing with water, the purity of the final product was inspected by using thin-layer chromatography and a fluorescence indicator. To separate the final product, column chromatography with a 4:6 ratio of ethyl acetate and hexane solvent mixture was utilized. Other compounds (**1b−l**) too were synthesized as described above.

Synthesis of Compound 2a. The compound **2a** was prepared by combining 0.5 mol of compound **1a** with 0.01 mol (1.32 g) of cinnamaldehyde, 0.50 equiv of copper(II)-acetylacetonate, and $CHCl_3$ stirred at 10 h in room

https://doi.org/10.1021/acsomega.4c09524
ACS Omega 2025, 10, 1643−1656

Scheme 1. Synthetic Route of 1*H*-Pyrazolo[3,4-*b*]pyridine Derivatives 2a−l

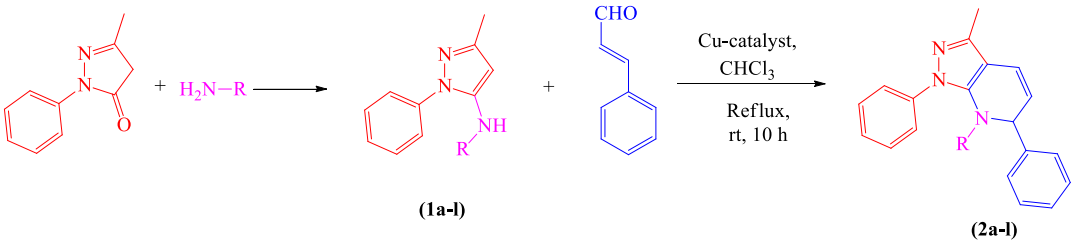

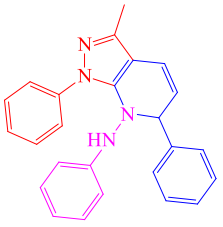

2a
Light green solid, 91%
$C_{25}H_{22}N_4$ (378.47 g/mol)
Mp: 170-172° C, R_f = 0.38

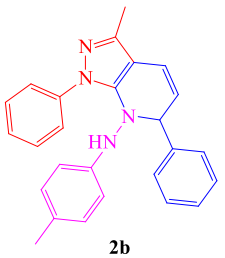

2b
White solid, 87%
$C_{26}H_{24}N_4$ (390.20 g/mol)
Mp: 176-178° C, R_f = 0.41

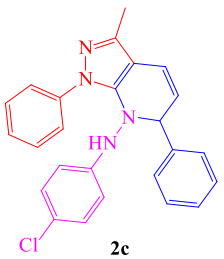

2c
Light white solid, 89%
$C_{25}H_{21}ClN_4$ (412.91 g/mol)
Mp: 162-164° C, R_f = 0.49

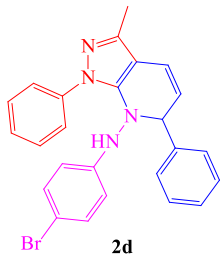

2d
Brown solid, 82%
$C_{25}H_{21}BrN_4$ (457.37 g/mol)
Mp: 180-182° C, R_f = 0.57

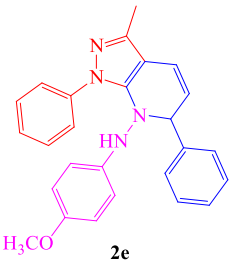

2e
Brown solid, 82%
$C_{26}H_{24}N_4O$ (408.49 g/mol)
Mp: 196-198° C, R_f = 0.35

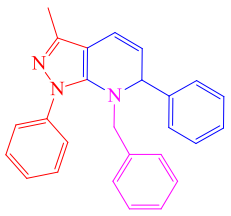

2f
Light brown solid, 90%
$C_{26}H_{23}N_3$ (377.48 g/mol)
Mp: 182-184° C, R_f = 0.32

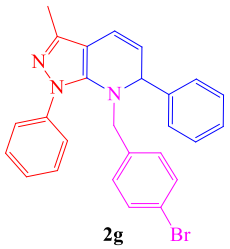

2g
Light brownsolid, 87%
$C_{26}H_{22}BrN_3$ (455.10 g/mol)
Mp: 181-183° C, R_f = 0.52

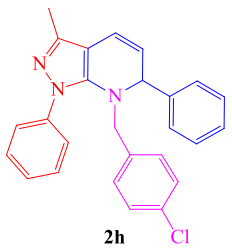

2h
White solid, 89%
$C_{26}H_{22}ClN_3$ (411.15 g/mol)
Mp: 161-163° C, R_f = 0.57

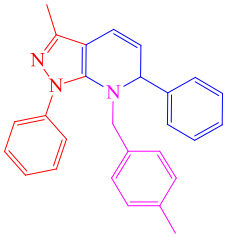

2i
Dark brown solid, 90%
$C_{27}H_{25}N_3$ (391.20 g/mol)
Mp: 182-184° C, R_f = 0.59

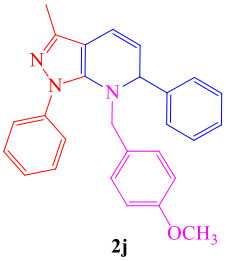

2j
Light brown solid, 87%
$C_{27}H_{25}N_3O$ (407.20 g/mol)
Mp: 167-169° C, R_f = 0.57

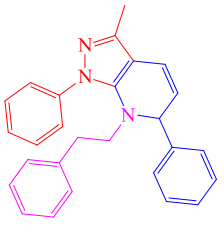

2k
Brown solid, 87%
$C_{27}H_{25}N_3$ (391.51.20 g/mol)
Mp: 153-155° C, R_f = 0.45

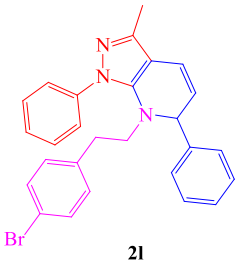

2l
Light brown solid, 93%
$C_{27}H_{24}BrN_3$ (470.40 g/mol)
Mp: 182-184° C, R_f = 0.38

temperature. Under a vacuum, the solution was concentrated, and 50 cm^3 of water was added. Ethyl acetate was used to extract the combination, which was then rinsed with a $NaHCO_3$ solution. Using concentrated Na_2SO_4 under low pressure, the crude residue was separated from the organic layer. The solid material obtained after filtration and dissolved in a 4:6 mixture of ethyl acetate and hexane was separated by using column chromatography. The same approach was employed for the other compounds (**2b−l**). Detailed physical values, spectral, mass, and analytical values of compounds (**2a−l**) are reported in the Supporting Information file.

Biological Activity. *Antibacterial Activity.* Synthesized compounds (**2a−l**) were screened for in vitro antibacterial activity against a battery of five WHO-prioritized drug-resistant Gram-positive (*VRE* and *MRSA*) and Gram-negative bacteria (*PRPA, ESBLKP,* and *ESBLEC*) via a disc diffusion technique. Bioassay was carried out by using the same methodology as described in our previous study.[42]

Cytotoxic Activity. A previously described method was employed to inspect the cytotoxicity of the synthesized compounds (**2a−l**).[43,44] The detailed experimental method is given in Supporting Information.

https://doi.org/10.1021/acsomega.4c09524
ACS Omega 2025, 10, 1643−1656

Scheme 2. Plausible Mechanism of Synthesis of 1*H*-Pyrazolo[3,4-*b*]pyridine Derivatives (2a−l)

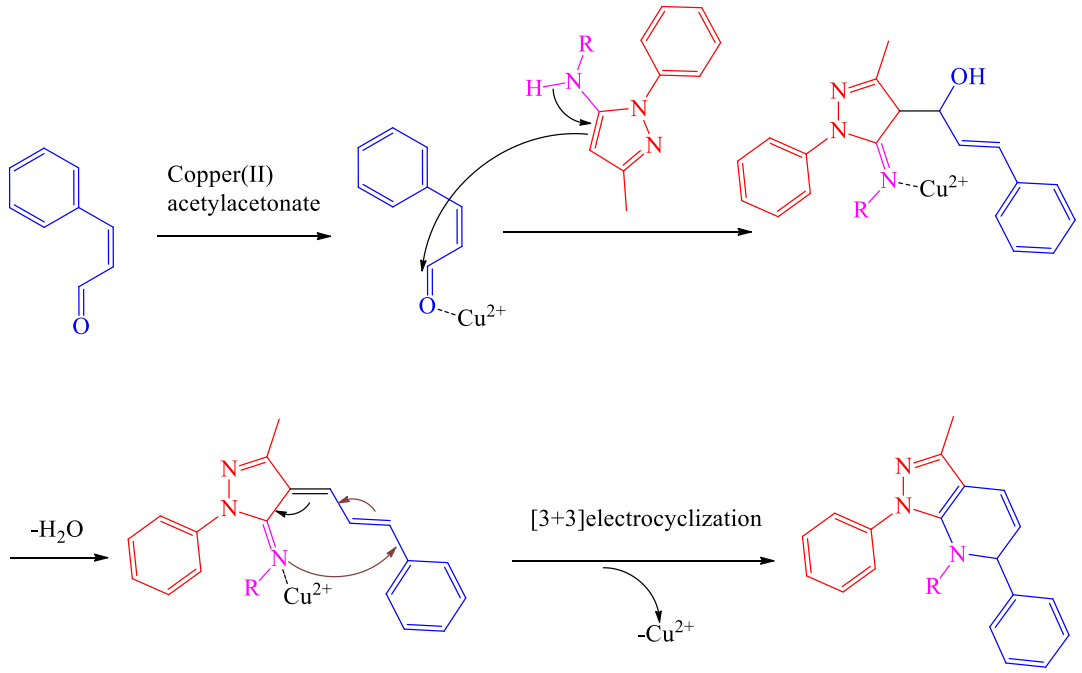

Computational Studies. *Molecular Docking Studies.* AutoDock Vina was employed using the standard protocol to dock compound **2g** against the active site of the protein (ID: 3G7B and 5UII). Molecular docking investigations were conducted using AutoDock Tools (ADT), a cost-free graphical user interface (GUI) for the AutoDock Vina program (http://mgltools.scripps.edu). ChemDraw 12 and ChemDraw3D pro were used to draw the ligand (http://www.cambridgesoft.com/). The proteins were downloaded from PDB (http://www.rcsb.org/). Postdocking analyses were performed using AutoDock Tools and Discovery Studio 2019, and the conformation with the lowest free binding energy was selected to examine the interactions between the target receptor and ligands via Discovery Studio.[45]

DFT Calculation. The molecular structure was determined using Gauss View 6.0.16. Figure 2 shows the atomic number of compound **2g**. The entire molecular geometry of the compound was optimized using the 6-31GI(d,p) basis set and density functional theory at the B3LYP level using the Gaussian 09 W software package. Based on the optimized structure of the compound, Gaussian 09 W software was utilized to calculate the molecular electrostatic potential, lowest unoccupied molecular orbital energy (LUMO), and highest occupied molecular orbital energy (HOMO).[46,47]

SwissADME Properties. To evaluate the predicted profiles of the synthesized compounds, we carried out in silico research that entailed computer predictions of physicochemical attributes. SwissADME servers were used to predict physicochemical properties based on Lipinski's five criteria.[48] The software was accessed in May 2024 (https://www.swissadme.ch/).

RESULTS AND DISCUSSION

Chemistry. Compounds **1a−l** were prepared by heating the respective pyrazolones with amines (Scheme 1) according to a previously reported procedure.[49] Pyrazolo[3,4-*b*]pyridine derivatives were synthesized in the presence of a Cu(II) acetylacetonate catalyst in a $CHCl_3$ medium via a formal cycloaddition reaction. The specific synthesis of pyrazolo[3,4-*b*]pyrimidine derivatives using Cu(II)acetylacetonate catalysis has not been previously documented in the existing literature. Compound **2a−l** was obtained in 85−90% yields. Scheme 1 shows the synthesis pathway and the mechanism of preparation of compounds (**2a−l**) shown in Scheme 2. According to a previously reported literature, it followed a plausible mechanism.[50]

Table 1. Optimization of Solvent Using Synthesis of Compound 2a[a]

entry	solvent	condition	yield [%]
1	acetonitrile	rt, 15 h	20
2	methanol	rt, 15 h	0
3	ethanol	rt, 15 h	0
4	benzene	rt, 15 h	40
5	toluene	rt, 10 h	68
6	$CHCl_3$	rt, 10 h	94
7	*n*-hexane	reflux, 65 °C, 10 h	43
8	CH_2Cl_2	rt, 10 h	85
9	THF	reflux, 65 °C, 10 h	30
10	dichloroethane	reflux, 70 °C, 10 h	52

[a]Note: rt-room temperature.

Formal [3 + 3] cycloaddition was performed to prepare pyridine-7-(6*H*)-amine **2a**. The product yield was 20% when acetonitrile was used as the solvent under reflux. Methanol and ethanol were unproductive (Table 1, entries 1−3), whereas the yield was enhanced to 40% in benzene (Table 1, entry 4). However, the Cu(II)acetylacetonate catalyst in various solvents, that is, toluene, $CHCl_3$, *n*-hexane, CH_2Cl_2, THF, and dichloroethane at room temperature, yielded product **2a** in higher percentages of 68, 94, 43, 85, 30, and 52%, respectively. Table 1 shows the solvent optimization of the synthesized compound **2a**.

Optimization of various Cu(II) catalysts was used for the reaction, and 20−94% of the products were obtained (entries

https://doi.org/10.1021/acsomega.4c09524
ACS Omega 2025, 10, 1643−1656

Table 2. Optimization of Various Cu(II) Catalysts on Synthesized Compound 2a[a]

entry	catalysis	temp.	solvent	equiv	time [h]	% yield
1	$CuCl_2$	rt	$CHCl_3$	0.50	48	20
2	dichloro(1,10-phenanthroline)copper(II)	rt	$CHCl_3$	0.50	24	38
3	copper(II) *tert*-butyl acetoacetate	rt	$CHCl_3$	0.50	16	47
4	copper(II) acetate	rt	$CHCl_3$	0.50	10	88
				0.10	10	80
				0.05	10	65
				0.01	10	58
5	copper(II) acetylacetonate	rt	$CHCl_3$	0.50	10	94
				0.10	10	94
				0.05	10	82
				0.01	10	74
6	ammonium tetrachlorocuprate(II) dehydrate	rt	$CHCl_3$	0.50	16	37
7	copper(II)ethyl acetoacetate	rt	$CHCl_3$	0.50	10	80
				0.10	10	60
				0.05	10	50
				0.01	10	20
8	copper(II) oxide	rt	$CHCl_3$	0.50	24	33
9	$CuSO_4$	rt	$CHCl_3$	0.50	24	42
10	**$Cu(OTf)_2$**	rt	$CHCl_3$	0.50	24	66

[a]Note: rt-room temperature.

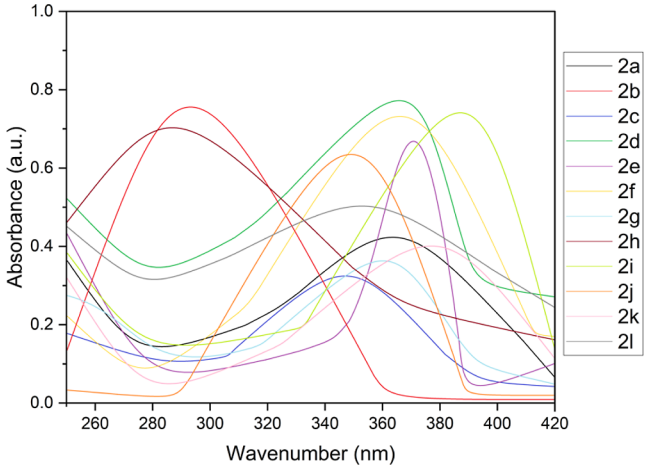

Figure 3. UV−visible spectra of compounds **2a−l**.

Table 3. Compounds (2a−l): MIC (μg/mL)[a]

compound no.	antibacterial activity				
	Gram-positives			Gram-negatives	
	VRE	*MRSA*	*PRPA*	*ESBLKP*	*ESBLEC*
2a	64	64	64	64	32
2b	64	64	>100	64	32
2c	64	8	64	32	16
2d	>100	>100	64	64	64
2e	>100	>100	>100	64	>100
2f	32	8	>100	32	8
2g	8	2	4	16	4
2h	64	>100	64	32	>100
2i	64	>100	64	>100	>100
2j	8	4	>100	16	8
2k	64	>100	64	>100	>100
2l	16	64	8	8	4
ciprofloxacin	16	4	8	16	8

[a]Note: VRE: vancomycin-resistant Enterococci, MRSA: methicillin-resistant *Staphylococcus aureus*, PRPA: piperacillin-resistant *Pseudomonas aeruginosa*, ESBLEC: ESBL producing *E. coli*, and ESBLKP: ESBL-producing *Klebsiella Pneumoniae*.

1−10 in Table 2). The catalyst Cu(II) acetylacetonate (0.5 equiv), when used at room temperature, provided a high yield (94%) when the reaction was carried out in $CHCl_3$ under reflux conditions at room temperature for a maximum of 48 h (Table 1, entry 6). In addition, the yield obtained using 0.1 equiv of this catalyst was much higher (94%, entry 5, Table 2) than that obtained using a much higher proportion of the other catalysts (0.5 equiv). Table 2 shows the optimization of the catalyst effect on the synthesized compound **2a**. As for experiment usage for catalyst 0.01 equiv, the product yield was 74%, and when we used the catalyst 0.1 equiv, the product yield increased to 94%. When the amount of catalyst was tried to 0.5 equiv, the product yield was 94% only; therefore, 0.1 equiv was more suitable for this reaction.

Spectral Characterization of 2a−l. FTIR, NMR, mass spectrum analysis, and elemental analysis were used to characterize the synthesized compounds. The −NH, C−N, N−H bending, and −C═C groups exhibited absorption bands at 3340−3349, 1078−1091, 1600−1611, and 1400−1408 cm^{-1} in the IR spectra of **2a−l**. The ^{1}H NMR spectra of **2a−l** show a peak at δ 4.0−4.2, corresponding to the presence of −NH. The peak at δ 4.54−4.59 corresponds to the presence of CH protein. Peaks at δ 2.46−2.47 indicate the existence of the $-CH_3$ group, and δ 6.0−6.32 and 6.32−6.24 correspond to the presence of the −CH═CH moiety in pyridine. The **2a−l** ^{13}C NMR spectrum revealed peaks at δ 145.2−143.9, 143.1−143.9, 129.0−129.9, 135.1−135.5, 121.0−121.6, 71.0−71.9, and 14.1−14.5, corresponding to −C═N in the pyrazole moiety, −C−C is the connecting pyridine moiety, −C−C is the connecting pyridine moiety in the presence of pyridine, −C═C moiety, −C═C in the presence of pyridine moiety, −CH presence of pyridine moiety, and $-CH_3$ attached to the pyrazole moiety, respectively. The compound **2a** m/z molecular ion peak at 356.75 was identified from the mass spectra; the other compounds, **2a−l**, were also confirmed by

https://doi.org/10.1021/acsomega.4c09524
ACS Omega 2025, 10, 1643−1656

Table 4. Compounds (2a−l): Cytotoxicity Activity[a]

compounds	HepG2 (μM)			MCF-7 (μM)		
	GI_{50}	TGI	LC_{50}	GI_{50}	TGI	LC_{50}
2a	13.2 ± 0.65	26.1 ± 0.09	56.4 ± 0.05	5.6 ± 0.65	10.1 ± 0.09	21.0 ± 0.16
2b	26.9 ± 0.43	59.4 ± 0.16	91.8 ± 0.05	35.9 ± 0.43	67.4 ± 0.16	>100
2c	5.21 ± 0.23	10.52 ± 0.32	25.28 ± 0.17	2.96 ± 0.23	6.28 ± 0.32	12.36 ± 0.17
2d	35.2 ± 0.19	70.1 ± 0.22	>100	15.2 ± 0.19	30.1 ± 0.22	62.2 ± 0.32
2e	14.5 ± 0.13	29.6 ± 0.12	71.2 ± 0.43	33.5 ± 0.13	66.6 ± 0.12	>100
2f	0.05 ± 0.65	0.81 ± 0.09	1.05 ± 0.20	0.01 ± 0.65	0.36 ± 0.09	0.65 ± 0.05
2g	0.01 ± 0.43	0.17 ± 0.16	0.55 ± 0.05	0.03 ± 0.43	0.94 ± 0.16	1.25 ± 0.05
2h	22.9 ± 0.23	48.0 ± 0.32	86.0 ± 0.17	21.9 ± 0.23	47.0 ± 0.32	87.0 ± 0.17
2i	55.2 ± 0.19	>100	-	22.2 ± 0.19	44.0 ± 0.22	81.02 ± 0.17
2j	0.01 ± 0.13	1.52 ± 0.12	2.65 ± 0.17	0.01 ± 0.13	0.26 ± 0.12	0.82 ± 0.17
2k	8.2 ± 0.65	16.1 ± 0.09	>100	8.2 ± 0.65	16.1 ± 0.09	>100
2l	0.01 ± 1.17	0.45 ± 0.27	0.60 ± 0.97	0.02 ± 0.17	0.28 ± 0.97	0.80 ± 0.77
doxorubicin	0.01 ± 0.41	0.13 ± 0.60	0.58 ± 0.81	0.02 ± 0.60	0.21 ± 0.59	0.74 ± 0.31

[a]Values are expressed in means ± SD; - no active.

Table 5. Molecular Docking Result of Compound 2g with 3G7B and 5UII Proteins[a]

protein id	3G7B (methicillin resistant S. aureus)		5UII (ESBL producing E. coli)	
compounds	**2g**	ciprofloxacin	**2g**	ciprofloxacin
binding energy (kcal/mol)	−8.5	−7.3	−10.0	−8.4
H-bond residues	-	-	-	3 (ILE^5, ALA^7, TYR^{100})

[a]Note: - no interaction.

mass spectrometry. The detailed ^1H and ^{13}C NMR spectra are shown in the Supporting Information file (Figures S1−S24).

The UV−vis spectra of pyrazolo[3,4-*b*]pyridine derivatives (**2a−l**) were investigated by using a PC-based double-beam spectrophotometer 2202. The absorption spectrum of **2a** exhibited a peak at 365 nm, with its absorption band extending beyond 410 nm. This range nearly matched that of previously reported pyrazolo[3,4-*b*]pyridine derivatives.[51] Highly active compound **2g** showed an absorbance range of 357 nm. Some compounds showed lower observed excitation. The reduced level of excitation observed might be attributed to certain limitations in the ability of the molecule to transfer charge.[52] The maximum absorption wavelengths were found to be of greater magnitude for compounds **2b** (298 nm), **2e** (369 nm), **2i** (392 nm), and **2j** (350 nm) due to the potent electron-donating properties of the $-CH_3$ and $-OCH_3$ groups located at the para position on the benzene ring. The absorbance ranges of other compounds **2c**, **2d**, **2f**, **2h**, **2k**, and **2l** correspond to 285−379 nm. Figure 3 shows the UV−vis spectra of compounds **2a−l**.

Antibacterial Activity. The increasing threat of microorganisms becoming resistant to antibacterial agents is a significant public health challenge. It is essential to tackle this issue, as many infectious bacteria are now resistant to commonly prescribed antibiotics.[35] The study was intended to identify novel antibacterial agents that can effectively impede the growth of bacteria. Five WHO-prioritized drug-resistant Gram-positive and Gram-negative bacteria were used to test the in vitro antibacterial activity of the synthesized compounds. Compounds **2g** and **2j** exhibited significant inhibitory activity against vancomycin-resistant Enterococcus (VRE) at a concentration of 8 μg/mL, which is better than the standard at 16 μg/mL. Additionally, compounds **2g** and **2l** showed high activity at 4 μg/mL, while compounds **2f** and **2j** demonstrated equipotent activity at 8 μg/mL against extended-spectrum β-lactamase-producing *Escherichia coli* (ESBLEC) when compared to ciprofloxacin, which is also active at 8 μg/mL. Compound **2g** demonstrated exceptional activity at a concentration of 2 μg/mL against MRSA, while compound **2j** exhibited comparable activity at 4 μg/mL, which matches the standard of 4 μg/mL. For PRPA, compound **2g** was highly active at 4 μg/mL, and **2l** showed equivalent activity at 8 μg/mL, consistent with the standard of 8 μg/mL. Regarding ESBLKP, compound **2l** was highly active at 8 μg/mL, whereas compound **2g** had equivalent activity at 16 μg/mL compared to the standard of 16 μg/mL. The details of the minimum inhibitory concentration (MIC) values for the synthesized derivatives (**2a−l**) are presented in Table 3.

Cytotoxic Activity. Cytotoxicity assays are commonly performed to assess the potential toxicity of test compounds, especially those intended for use in pharmaceuticals or cosmetics, where minimal to no toxicity is crucial.[53] The cytotoxic activity of compounds (**2a−l**) was examined against HepG2 and MCF-7 cell lines using an MTT anticancer assay. The cytotoxic activity results are listed in Table 4. Total growth inhibition (TGI), growth inhibitory concentration (GI_{50}), and lethal concentration (LC_{50}) were used to describe the results. Compounds **2j** (GI_{50} = 0.01 ± 0.13 μM) and **2l** (GI_{50} = 0.01 ± 0.17 μM) were highly active than doxorubicin (GI_{50} = 0.01 ± 0.41 μM) against HepG2 cell line, whereas compound **2g** was highly active in GI_{50} (0.01 ± 0.43 μM), and nearly equal active in TGI (0.17 ± 0.16 μM), LC_{50} (0.55 ± 0.05 μM) against HepG2 cell line than standard (GI_{50} = 0.01 ± 0.41 μM, TGI = 0.13 ± 0.60 μM, and LC_{50} = 0.58 ± 0.81 μM).

In the case of MCF-7 cell line, compounds **2f** (GI_{50} = 0.01 ± 0.65 μM) and **2j** (GI_{50} = 0.01 ± 0.13 μM) were highly active, **2l** (GI_{50} = 0.02 ± 0.17 μM) was equipotential active, and **2g** (GI_{50} = 0.03 ± 0.43 μM) was nearly equipotential active than standard (GI_{50} = 0.02 ± 0.60 μM). The compound **2f** (LC_{50} = 0.65 ± 0.05 μM) was more active than the standard (GI_{50} = 0.74 ± 0.31 μM), whereas **2j** (TGI = 0.26 ± 0.12 μM) was almost equally active than doxorubicin (TGI = 0.21 ± 0.59 μM).

Molecular Docking. Molecular docking is a highly effective computational method in the field of drug discovery,

https://doi.org/10.1021/acsomega.4c09524
ACS Omega 2025, 10, 1643−1656

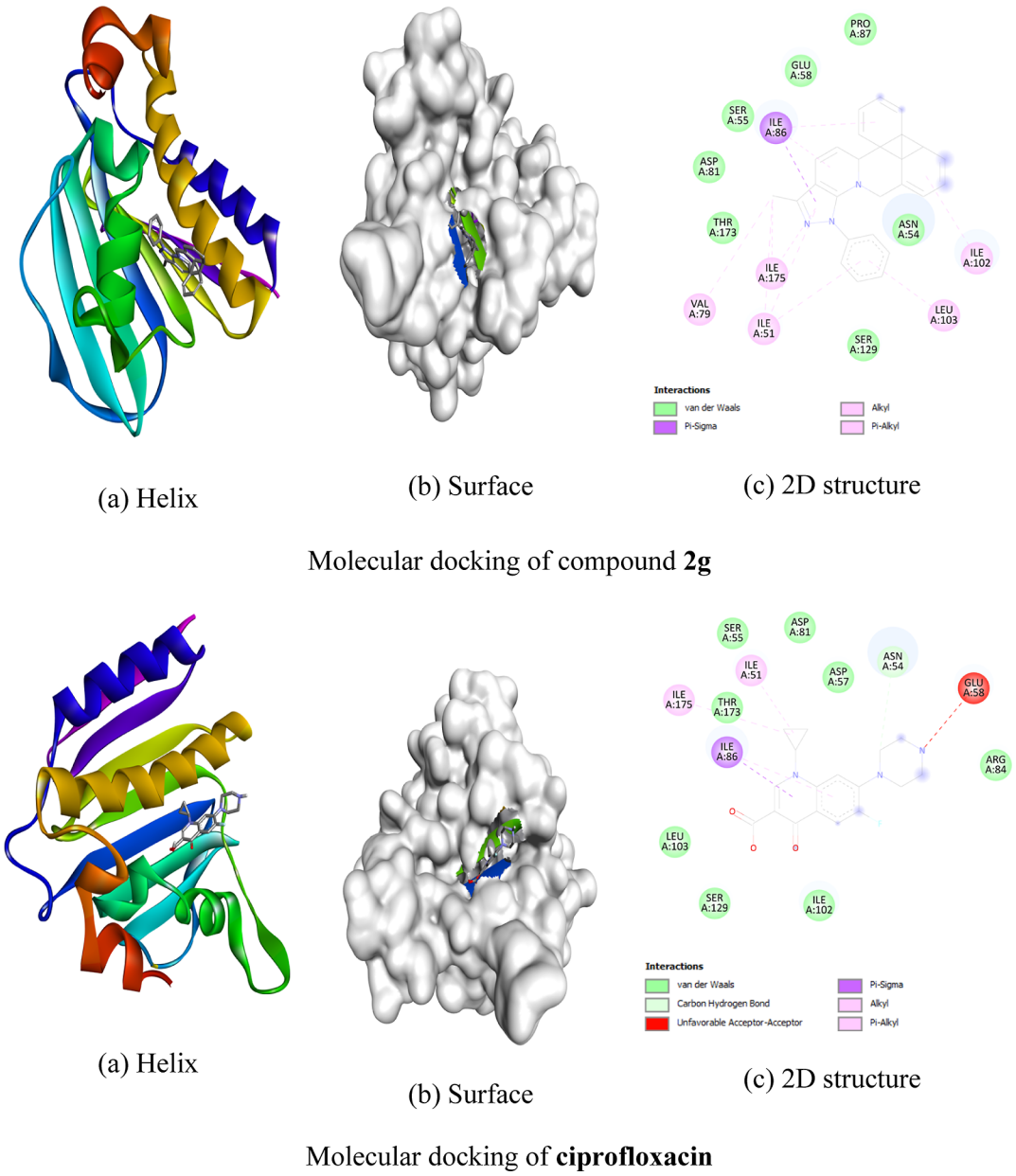

Figure 4. Molecular docking result of compound **2g** and ciprofloxacin with the 3G7B protein.

as it allows researchers to predict the interactions between small-molecule ligands and their target proteins. This method has been widely acknowledged for its capacity to expedite the drug development process by effectively screening extensive chemical libraries and identifying prospective lead compounds.[54−57] In this study, the highly active antibacterial activity compound **2g** was investigated in a molecular docking study.

The protein 3G7B (methicillin-resistant *S. aureus*) was selected from the previously reported literature.[58] The construction of the grid box involved the use of 20 units in the *x*-, *y*-, and *z* directions, with a spacing of 0.375 Å between each grid point. The center of the grid box was located at x = 50.354241 Å, y = −2.963621 Å, and z = 19.128759 Å. The compound **2g** had higher binding affinity compared to ciprofloxacin −8.5 vs −7.3 kcal/mol, interaction of the 3G7B protein (Table 5). The compound **2g** interaction residues are van der Waals bonds (ASN^{54}, SER^{55}, GLU^{58}, ASP^{81}, PRO^{87}, SER^{129}, THR^{173}), alkyl, pi-alkyl bonds (ILE^{51}, VAL^{79}, ILE^{102}, LEU^{103}, ILE^{175}), and pi-Sigma bonds (ILE^{86}). The standard interaction residue are van der Waals bonds (ASP^{55}, ASP^{57}, ASP^{81}, ASP^{84}, ILE^{102}, LEU^{103}, SER^{129}, and THR^{173}), conventional H-bonds (ASN^{54}), alkyl, pi-alkyl bonds (ILE^{51}, ILE^{175}), pi−sigma bonds (ILE^{86}), and unfavorable acceptor−acceptor bond (GLU^{58}). Figure 4 shows the detailed ligand and residue interactions in compound **2g** and the standard with the protein.

Previously reported literature-based protein 5UII (ESBL-producing *E. coli*) was selected.[59] The grid box and grid point parameters followed the above results. The center of the grid box was located at x = 14.256786 Å, y = 11.210271 Å, and z = 14.286914 Å. In the results, compound **2g** was more active than standard (−10.0 vs −8.4 kcal/mol). Table 5 shows the results. The **2g** interaction residues are van der Waals bonds (GLY^{15}, ALA^{19}, THR^{46}, SER^{49}, ILE^{94}, GLY^{95}, GLY^{96}, GLY^{97}, and THR^{123}) and alkyl, Pi−alkyl bonds (ILE^{14}, MET^{20}, PHE^{31},

https://doi.org/10.1021/acsomega.4c09524
ACS Omega 2025, 10, 1643−1656

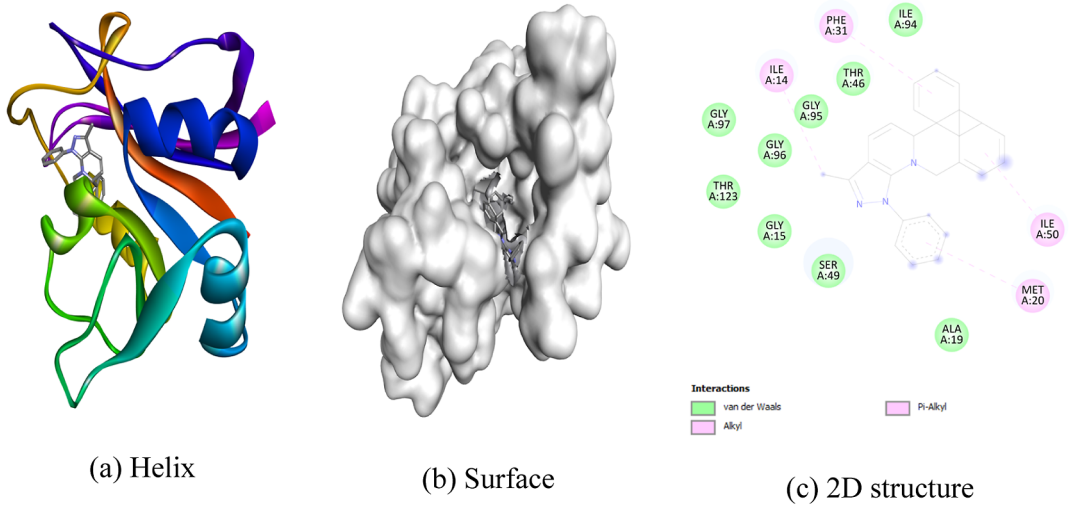

Figure 5. Molecular docking result of compound **2g** and ciprofloxacin with 5UII protein.

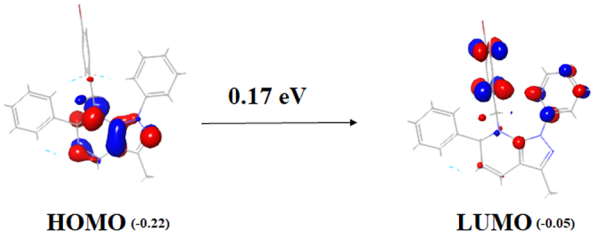

Figure 6. HOMO−LUMO energy gap (ΔE) of compound **2g**.

ILE[50]). The standard interaction residues were three H-bond interactions (ILE[5], ALA[7], and TYR[100]), van der Waals bonds (GLY[15], HIS[45], ALA[6], PHE[31], THR[46], SER[49], ILE[94], GLY[95], GLY[96], GLY[97], and THR[123]), conventional H-bonds (MET[16]), amide-pi stacked (ILE[14]), and alkyl and Pi−alkyl bonds (ILE[50]). The interaction of the ligand−protein and residues is shown in Figure 5.

Frontier Molecular Orbitals. Research on the frontier molecular orbital (FMO) has primarily focused on illuminating various facets of chemical reactivity, including the LUMO and HOMO. Recently, there has been a focus on how the FMOs of a material affect its biological reactivity. FMOs have been linked to a variety of biological characteristics, including anticancer, cytotoxic, antibacterial, and antifungal capabilities,

Table 6. FMO Energy and Chemical Reactivity of Compound 2g

properties	**2g** (eV)
HOMO	−0.22
LUMO	−0.05
ΔE	0.17
I	0.22
A	0.05
η	0.085
s	11.76
μ	−0.135
χ	0.135
ω	0.107
N	9.34

https://doi.org/10.1021/acsomega.4c09524
ACS Omega 2025, 10, 1643−1656

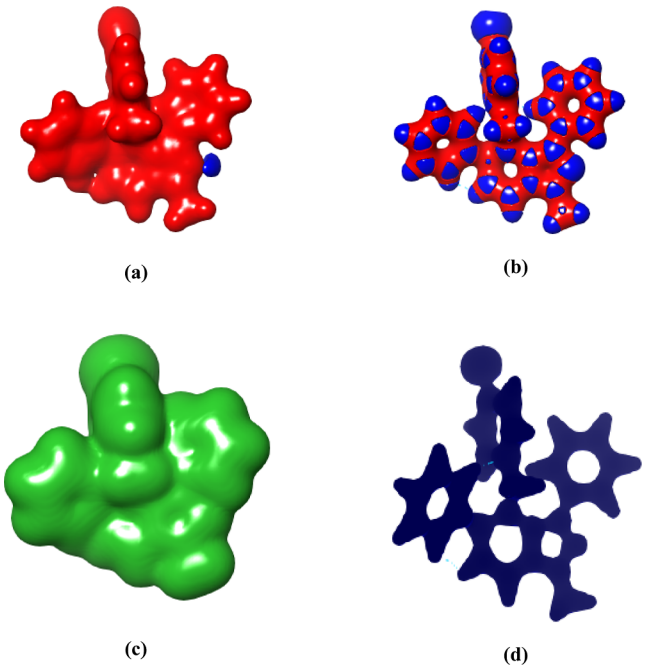

Figure 7. (a) Electrostatic potential, (b) interaction strength, (c) electron density, and (d) density application of compound **2g**.

Table 7. Physicochemical Properties of Synthesized Compounds (2a–l)[a]

compound	physico-chemical properties					Lipinski's five rules
	MW	MR index	log *P*	HBA	HBD	
rule	≤500 (g/mol)	130≥ MR index ≥40	<5	≤10	<5	(yes/no)
2a	378.47	122.16	3.51	1	1	yes
2b	392.50	127.12	3.75	1	1	yes
2c	412.91	127.17	3.68	1	1	yes
2d	457.37	129.86	3.88	1	1	yes
2e	408.49	128.65	3.79	2	1	yes
2f	377.48	122.62	3.76	1	0	yes
2g	456.38	130.32	4.11	1	0	yes
2h	411.93	127.63	3.95	1	0	yes
2i	405.53	132.40	4.27	1	0	yes
2j	407.51	129.11	4.01	2	0	yes

[a]Note: MW-molecular weight; MR index-molar refractivity index; HBA–hydrogen bond acceptors, and HBD–hydrogen bond donors.

according to several studies.[60−65] This indicates that the area of drug design is rapidly expanding.[66]

The energy gaps and levels of the FMOs (εHOMO, εLUMO, and ΔE) may be used to study two important parameters: the potential required for ionization from the HOMO level ($I = -\varepsilon\text{HOMO}$) and the electron affinity obtained from the energy of the LUMO ($A = -\varepsilon\text{LUMO}$). The compound **2g** energy gap is 0.17 eV (Figure 6). Moreover, FMOs demonstrate remarkable performance in assessing a range of chemical reactivity descriptors, including electrophilicity (ω), global hardness (η), electronegativity (χ), and softness (δ; Table 6). These parameters were computed using the following formulas

$$\Delta E = \text{LUMO} - HOMO \tag{1}$$

$$\eta = \frac{(I - A)}{2} \tag{2}$$

$$s = \frac{1}{\eta} \tag{3}$$

$$\mu = -\frac{(I + A)}{2} \tag{4}$$

$$\chi = -\mu \tag{5}$$

$$\omega = \frac{\mu^2}{2\eta} \tag{6}$$

$$N = \frac{1}{\omega} \tag{7}$$

Calculating the MEP (molecular electrostatic potential) may be crucial for confirming data supporting the inhibitory interactions of these chemicals. The MEP provides information about the magnitude and form of the electrostatic potential and may be utilized as a method for forecasting physicochemical characteristics related to the molecule structure. Nucleophilic and electrophilic assays of the compound were performed using MEP. Using the same methodology and basis sets, the MEP for compound **2g**, which showed the greatest binding affinity, was ascertained. The (a) electrostatic potential, (b) interaction strength, (c) electron density, and (d) density application are shown in Figure 7.

SwissADME Physicochemical Properties. In silico, computational research has expedited and lowered the cost of tests before any clinical trial. The technique is of interest to many and is widely documented in the literature.[67] Lipinski's rule of five (Ro5) is a qualitative approach that is employed in the field of drug discovery to evaluate the drug ability of compounds and ascertain whether they possess the necessary properties to be orally effective in humans. Most oral medications that work well are tiny and somewhat lipophilic, which is the premise of this rule.[68,69]

The synthesized compounds were examined to ensure that they followed Lipinski's five criteria and were comparable to medication prospects. In this regard, we observed that the synthesized compounds were expected to be small molecules, with maximal numbers of 5 and 10 H-bond donors and acceptors, respectively, for each compound, and MR indices ranging from 130≥ to ≥40. They were also expected to have lipophilicity less than 5 log *P*. Thus, as Table 7 illustrates, the synthesized compounds show striking resemblances to therapeutic candidates.

Correlation between Biological Activities with Computational Studies. Investigation of compounds binding to bacterial targets through molecular docking techniques can elucidate their antibacterial properties. Moreover, the application of molecular docking analyses to synthesized compounds has revealed promising interactions with specific targets, offering valuable insights into potential mechanisms of action.[70,71]

According to computational studies, the active compound of **2g** was more active against Gram-positive (MIC: 2 μg/mL) and Gram-negative (MIC: 4 μg/mL) bacteria than the standard (MIC: 4 and 8 μg/mL), whereas **2g** was nearly equally cytotoxic as the standard. The compound was subjected to molecular docking studies using the 3G7B, 5UII, and 4FM9 proteins. Compound **2g** had a higher binding

https://doi.org/10.1021/acsomega.4c09524
ACS Omega 2025, 10, 1643−1656

Table 8. Correlation between the Biological Activities and Molecular Docking Results[a]

compounds	biological activity			molecular docking		
	antibacterial activity		cytotoxic activity	antibacterial activity		cytotoxic activity
	MARS (μg/mL)	ESBLEC (μg/mL)	MCF-7 (GI_{50})	3G7B (kcal/mol)	5UII (kcal/mol)	4FM9 (kcal/mol)
2a	64	32	5.6 ± 0.65	−7.6	−8.5	−7.6
2b	64	32	35.9 ± 0.43	−8.3	−8.3	−7.4
2c	8	16	2.96 ± 0.23	−8.0	−8.2	−7.6
2d	>100	64	15.2 ± 0.19	−8.1	−9.3	−7.4
2e	>100	>100	33.5 ± 0.13	−7.4	−9.4	−7.7
2f	8	8	0.01 ± 0.65	−6.7	−8.2	−6.5
2g	2	4	0.03 ± 0.43	−8.5	−10.0	−8.2
2h	>100	>100	21.9 ± 0.23	−7.2	−8.5	−6.0
2i	>100	>100	22.2 ± 0.19	−7.3	−8.5	−6.5
2j	4	8	0.01 ± 0.13	−8.2	−9.6	−7.9
2k	>100	>100	8.2 ± 0.65	−8.1	−9.4	−7.8
2l	64	4	0.02 ± 0.17	−8.0	−8.5	−7.8
ciprofloxacin	4	8	-	−7.3	−8.4	-
doxorubicin	-	-	0.02 ± 0.60	-	-	−7.5

[a]Note: - no activity; MRSA: methicillin-resistant *S. aureus*, ESBLEC: ESBL producing *E. coli*.

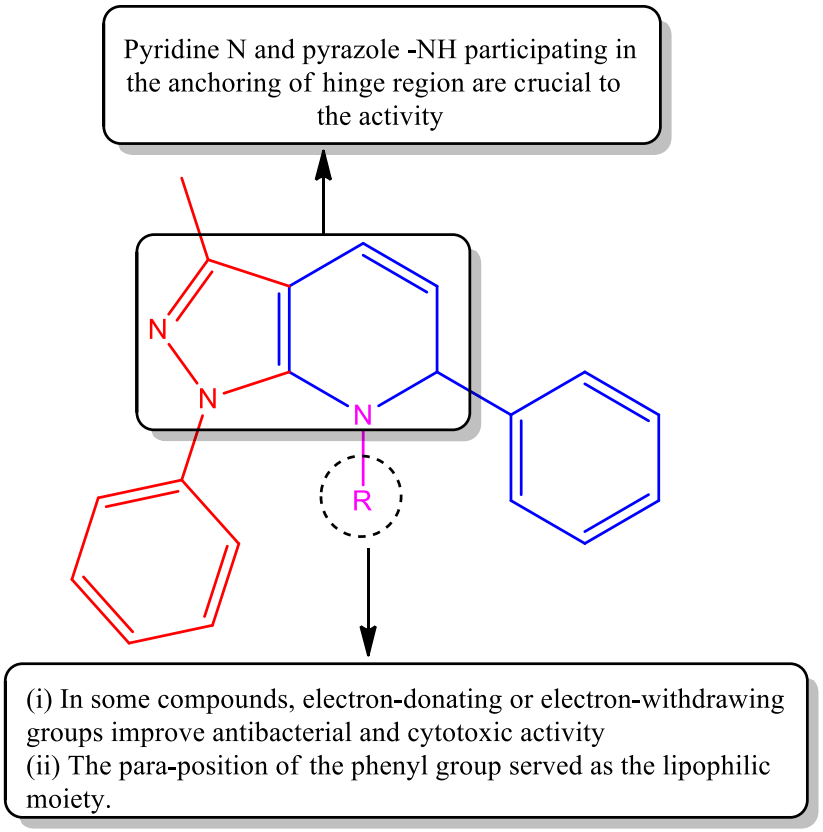

Figure 8. SAR of compound **2a**–**l**.

affinity than the standard against antibacterial (−8.5 vs −7.3 and −9.8 vs −8.4 kcal/mol) and cytotoxic activities (−8.2 vs −7.5 kcal/mol). Similarly, compound **2j** was equally active against antibacterial activity as the standard, whereas **2j** was more active than the standard in terms of cytotoxic activity. Compound **2j** was used for the computational study of molecular docking. Compound **2j** had a higher binding affinity than the standard for biological activities (−8.2 vs −7.3, −9.6 vs −8.4, and −7.9 vs −7.5 kcal/mol). The other compounds had lower biological activities than the standard, and molecular docking studies showed lower binding affinities. The correlation between biological activities and molecular docking results is shown in Table 8. The 3d structures of the molecular docking results are given in the Supporting Information file (Figures S25−S27).

Structural Activity Relationship. Structural activity relationship (SAR) can be used to establish the relationship between a molecule's chemical structure and its biological activity. This helps to pinpoint the key chemical group or atom responsible for adjusting the potency. Electron-donating (EDG) and electron-withdrawing (EWG) effects play a vital role in organic reactions as they significantly impact the

https://doi.org/10.1021/acsomega.4c09524
ACS Omega 2025, 10, 1643−1656

reactivity and behavior of molecules. It is essential to consider the effects that are fundamental in determining the nucleophile and electrophile strengths, which, in turn, affect the outcome and rate of various organic reactions. A crucial aspect of organic chemistry is understanding these concepts, which is indispensable for forecasting the outcomes of chemical reactions and formulating synthetic approaches.

In this study, the position of the phenyl group, in terms of its attachment to the main structure, acted as the source of the lipophilic properties. The core moiety of pyridine-N and pyrazole-NH participating in the anchoring of the hinge region is crucial to the activity.[72,73] The compounds **2g** and **2l** were highly active in antibacterial and cytotoxic activities. SAR analysis showed that the presence of EWG (−Br) improved antibacterial activity and demonstrated hydrophilic properties. Compound **2j** was highly cytotoxic, and EDG ($-OCH_3$) enhanced the cytotoxic activity. Figure 8 shows the SAR activity.

CONCLUSIONS

A novel pyrazole[3,4-*b*]pyridine (**2a**−**l**) derivative was synthesized via a formal [3 + 3] cycloaddition reaction using Cu(II) as a catalyst and refluxed in the presence of $CHCl_3$. The synthesized products were evaluated for their antibacterial and cytotoxic activities. Compounds **2g**, **2f**, and **2l** were significantly more active against drug-resistant bacteria than the positive control ciprofloxacin (MIC = 4 g/mL). Compounds **2f** and **2j** were relatively more active against the cell line MCF-7 than the other drugs (GI_{50} = 0.01 μM). Compounds **2g**, **2j**, and **2l** were noticeably more effective (GI_{50} = 0.01 μM) against HepG2 cancer cells. Highly active compound **2g** was investigated by using in silico molecular docking and DFT calculations. Compound **2g** had a higher docking score than that of the standard (−8.5 vs −7.3 and −10.0 vs −8.4 kcal/mol). In compound **2g**, the energy gap was 0.17 eV, as determined using DFT calculations. The physicochemical properties of all compounds were investigated using SwissADME. Overall, compound **2g** exhibited promising antibacterial and cytotoxic activities. Some in vitro and in vivo activities are required for **2g** to act as a multitarget agent.

ASSOCIATED CONTENT

Data Availability Statement

Data will be made available on request.

Supporting Information

The Supporting Information is available free of charge at https://pubs.acs.org/doi/10.1021/acsomega.4c09524.

Additional experimental details, NMR (^1H and ^{13}C) spectra, and molecular docking 3d structure for all compounds (PDF)

AUTHOR INFORMATION

Corresponding Author

Idhayadhulla Akbar − *Research Department of Chemistry, Nehru Memorial College (Affiliated to Bharathidasan University), Tiruchirappalli District, Tamil Nadu 621007, South India;* orcid.org/0000-0003-0309-6274; Email: a.idhayadhulla@gmail.com

Authors

Velmurugan Loganathan − *Research Department of Chemistry, Nehru Memorial College (Affiliated to Bharathidasan University), Tiruchirappalli District, Tamil Nadu 621007, South India*

Anis Ahamed − *Department of Botany and Microbiology, College of Science, King Saud University, Riyadh 11451, Saudi Arabia*

Desta Galcha Gerbu − *School of Medicine, College of Medicine and Health Sciences, Arba Minch University, Arba Minch 21, Ethiopia*

Hissah Abdulrahman Alodaini − *Department of Botany and Microbiology, College of Science, King Saud University, Riyadh 11451, Saudi Arabia*

Aseer Manilal − *Department of Medical Laboratory Sciences, College of Medicine and Health Sciences, Arba Minch University, Arba Minch 21, Ethiopia*

Complete contact information is available at: https://pubs.acs.org/10.1021/acsomega.4c09524

Author Contributions

Methodology, V.L.; formal analysis, A.A.; investigation, supervision, A.I.; spectral characterization, D.G.G.; Funding Acquisition, H.A.A.; software, A.M. The original draft of the manuscript was prepared through the collaborative efforts of everyone involved.

Notes

The authors declare no competing financial interest.

ACKNOWLEDGMENTS

The Government of India's Department of Science and Technology thanks the authors for supporting Nehru Memorial College with financial aid (instrumentation facility) via the FIST program (SR/FST/COLLEGE-372/2018), New Delhi, India. The authors extend their appreciation to the Researchers supporting project number (RSP2024R479), King Saud University, Riyadh, Saudi Arabia.

REFERENCES

(1) Kerru, N.; Gummidi, L.; Maddila, S.; Gangu, K. K.; Jonnalagadda, S. B. A review on recent advances in nitrogen-containing molecules and their biological applications. *Molecules* **2020**, *25* (8), 1909.

(2) Wang, W.; Xiong, L.; Li, Y.; Song, Z.; Sun, D.; Li, H.; Chen, L. Synthesis of lathyrane diterpenoid nitrogen-containing heterocyclic derivatives and evaluation of their anti-inflammatory activities. *Bioorg. Med. Chem.* **2022**, *56*, 116627.

(3) Govindaraju, S.; Tabassum, S.; Pasha, M. A. Meglumine catalyzed one-pot green synthesis of novel 4,7-dihydro-1H-pyrazolo-[3,4-b]pyridin-6-amines. *Chin. Chem. Lett.* **2017**, *28* (2), 437−441.

(4) Abdel-Monem, Y. K.; Abou El-Enein, S. A.; El-Sheikh-Amer, M. M. Design of new metal complexes of 2-(3-amino-4,6-dimethyl-1H-pyrazolo[3,4-b]pyridin-1-yl)aceto- hydrazide: Synthesis, characterization, modelling and antioxidant activity. *J. Mol. Struct.* **2017**, *1127*, 386−396.

(5) El Emary, T. I. Synthesis of Newly Substituted Pyrazoles and Substituted Pyrazolo[3,4 b]Pyridines Based on 5 Amino 3 Methyl 1 Phenylpyrazole. *J. Chin. Chem. Soc.* **2007**, *54* (2), 507−518.

(6) Ge, M.; Cline, E.; Yang, L. A general method for the preparation of 3-acyl-4-cyano-5- amino-pyrazoles. *Tetrahedron Lett.* **2006**, *47* (32), 5797−5799.

(7) El-Agrody, A. M.; Emam, H. A.; El-Hakim, M. H.; AbdEl-latif, M. S.; Fakery, A. H. Activated Nitriles in Heterocyclic Synthesis: Synthesis of Pyrano[2,3-d]pyrimidine and Pyrano[3,2-e][1,2,4]-triazolo[1,5-c]pyrimidine Derivatives. *J. Chem. Res.* **1997**, *9*, 320−321.

(8) Aly, A. A. Synthesis of polyfunctionally substituted pyrazolo-naphthyridine, pentaazanaphthalene, and heptaazaphenanthrene

https://doi.org/10.1021/acsomega.4c09524
ACS Omega 2025, 10, 1643−1656

derivatives. *Phosphorus, Sulfur, Silicon Relat. Elem.* **2006**, *181* (10), 2395−2409.
(9) Eissa, I. H.; El-Naggar, A. M.; El-Hashash, M. A. Design, synthesis, molecular modeling and biological evaluation of novel 1H-pyrazolo[3,4-b]pyridine derivatives as potential anticancer agents. *Bioorg. Chem.* **2016**, *67*, 43−56.
(10) Simha Pulla, R.; Ummadi, N.; Gudi, Y.; Venkatapuram, P.; Adivireddy, P. Synthesis and Antimicrobial Activity of Some New 3,4 Disubstituted Pyrroles and Pyrazoles. *J. Heterocycl. Chem.* **2018**, *55* (1), 115−124.
(11) Zhao, B.; Li, Y.; Xu, P.; Dai, Y.; Luo, C.; Sun, Y.; Ai, J.; Geng, M.; Duan, W. Discovery of substituted 1H-pyrazolo[3,4-b]pyridine derivatives as potent and selective FGFR kinase inhibitors. *ACS Med. Chem. Lett.* **2016**, *7* (6), 629−634.
(12) Aggarwal, R.; Kumar, S.; Sumran, G.; Sharma, D. One-pot synthesis and in vitro bioactivity of novel 4-aminopyrazolo[3,4-b]pyridine derivatives as potential antimicrobial compounds. *Med. Chem. Res.* **2024**, *33* (1), 117−126.
(13) Abdellatif, K. R.; Bakr, R. B. Pyrimidine and fused pyrimidine derivatives as promising protein kinase inhibitors for cancer treatment. *Med. Chem. Res.* **2021**, *30*, 31−49.
(14) Ribeiro, J. L.; Soares, J. C.; Portapilla, G. B.; Providello, M. V.; Lima, C. H.; Muri, E. M.; de Albuquerque, S.; Dias, L. R. Trypanocidal activity of new 1,6-diphenyl-1H-pyrazolo[3,4-b] pyridine derivatives: Synthesis, in vitro and in vivo studies. *Bioorg. Med. Chem.* **2021**, *29*, 115855.
(15) Al-Zharani, M.; Al-Eissa, M. S.; Rudayni, H. A.; Ali, D.; Alkahtani, S.; Surendrakumar, R.; Idhayadhulla, A. Pyrazolo[3,4-b]pyridin-3(2H)-one derivatives: Synthesis and their investigation of mosquito larvicidal activity. *J. King Saud Univ., Sci.* **2022**, *34* (2), 101767.
(16) Almansour, B. S.; Binjubair, F. A.; Abdel-Aziz, A. A. M.; Al-Rashood, S. T. Synthesis and In Vitro Anticancer Activity of Novel 4-Aryl-3-(4-methoxyphenyl)-1- phenyl-1H-pyrazolo[3,4-b]pyridines Arrest Cell Cycle and Induce Cell Apoptosis by Inhibiting CDK2 and/or CDK9. *Molecules* **2023**, *28* (17), 6428.
(17) Naglaa, F. M.; Rizk, S. A.; Galal, A. E.; Ali, A. K. Expeditious microwavable one-pot synthesis and biological exploration of spiro[indoline-3,4′-pyrazolo[3,4-b]pyridine derivatives. *J. Iran. Chem. Soc.* **2022**, *19* (8), 3711−3719.
(18) Desai, N.; Jadeja, D.; Mehta, H.; Khasiya, A.; Shah, K.; Pandit, U. Synthesis and Biological Importance of Pyrazole, Pyrazoline, and Indazole as Antibacterial, Antifungal, Antitubercular, Anticancer, and Anti-inflammatory Agents. In *N-Heterocycles: Synthesis and Biological Evaluation*; Springer Nature Singapore: Singapore, 2022; pp 143−189.
(19) Mehar, A.; Parvin, T. Synthesis of anthracene linked polycyclic pyridine derivatives fused with coumarin and pyrazole by one pot multi-component strategy followed by oxidation. *J. Heterocycl. Chem.* **2023**, *60* (8), 1437−1446.
(20) Miao, X. Y.; Hu, Y. J.; Liu, F. R.; Sun, Y. Y.; Sun, D.; Wu, A. X.; Zhu, Y. P. Synthesis of Diversified Pyrazolo[3,4-b]pyridine Frameworks from 5- Aminopyrazoles and Alkynyl Aldehydes via Switchable C≡C Bond Activation Approaches. *Molecules* **2022**, *27* (19), 6381.
(21) Kripalani, K. J.; Dreyfuss, J.; Nemec, J.; Cohen, A. I.; Meeker, F.; Egli, P. Biotransformation in the monkey of cartazolate(SQ 65,396), a substituted pyrazolopyridine having anxiolytic activity. *Xenobiotica* **1981**, *11* (7), 481−488.
(22) Bare, T. M.; McLaren, C. D.; Campbell, J. B.; Firor, J. W.; Resch, J. F.; Walters, C. P.; Salama, A. I.; Meiners, B. A.; Patel, J. B. Synthesis and structure-activity relationships of a series of anxioselective pyrazolopyridine ester and amide anxiolytic agents. *J. Med. Chem.* **1989**, *32* (12), 2561−2573.
(23) Kerru, N.; Gummidi, L.; Maddila, S.; Jonnalagadda, S. B. Efficient synthesis of novel functionalized dihydro-pyrazolo[3,4-d]pyridines via the three-component reaction using MgO/HAp as a sustainable catalyst. *Inorg. Chem. Commun.* **2021**, *123*, 108321.
(24) Warekar, P. P.; Patil, P. T.; Patil, K. T.; Jamale, D. K.; Kolekar, G. B.; Anbhule, P. V. PTSA-catalyzed straightforward novel approach for the synthesis of 1,2-bis (4- nitrophenyl)-1H-benzo[f]chromen-3-amine and the evaluation of their anti- tuberculosis activity. *Res. Chem. Intermed.* **2017**, *43*, 4115−4127.
(25) Safaei, S.; Mohammadpoor-Baltork, I.; Khosropour, A. R.; Moghadam, M.; Tangestaninejad, S.; Mirkhani, V.; Khavasi, H. R. One-Pot Three-Component Synthesis of Pyrano[3,2-b]pyrazolo[4,3-e]pyridin-8(1H)-ones. *ACS Comb. Sci.* **2013**, *15* (3), 141−146.
(26) Reddy, M. V.; Jeong, Y. T. Copper(ii)oxide nanoparticles as a highly active and reusable heterogeneous catalyst for the construction of phenyl-1H-pyrazolo[3,4-b] pyridine derivatives under solvent-free conditions. *RSC Adv.* **2016**, *6* (105), 103838−103842.
(27) Arlan, F. M.; Khalafy, J.; Maleki, R. One-pot three-component synthesis of a series of 4-aroyl-1,6-diaryl-3-methyl-1H-pyrazolo[3,4-b]pyridine-5-carbonitriles in the presence of aluminum oxide as a nanocatalyst. *Heterocycl. Chem.* **2018**, *54*, 51−57.
(28) Sepehrmansourie, H.; Zarei, M.; Zolfigol, M. A.; Babaee, S.; Azizian, S.; Rostamnia, S. Catalytic synthesis of new pyrazolo[3,4-b]pyridine via a cooperative vinylogous anomeric-based oxidation. *Sci. Rep.* **2022**, *12* (1), 14145.
(29) Mahdavinia, G. H.; Rahmati, A. Silica sulfuric acid as a solid acid catalyzed synthesis of 4,5,6,7-tetrahydro-2H-pyrazolo[3,4-b]-pyridine-5-carbonitriles and 1,4-diaryl-4,5- dihydro-3-methyl-1H-pyrazolo[3,4-b]pyridine-6(7H)-ones. *Rev. Roum. Chim.* **2015**, *60* (11−12), 1025−1032.
(30) Tavakoli, E.; Sepehrmansourie, H.; Zarei, M.; Zolfigol, M. A.; Khazaei, A.; As' Habi, M. A. Application of Zr-MOFs based copper complex in synthesis of pyrazolo[3,4-b] pyridine-5-carbonitriles via anomeric-based oxidation. *Sci. Rep.* **2023**, *13* (1), 9388.
(31) Zeleke, D.; Damena, T. Advance in green synthesis of pharmacological important heterocycles using multi-component reactions and magnetic nanocatalysts (MNCs). *Res. Chem.* **2024**, *7*, 101283.
(32) Satish, G.; Sharma, A.; Gadidasu, K. K.; Vedula, R. R.; Penta, S. Synthesis of 4-aryl- 2-pyranyl-7,8-dihydroquinolin-5(6 H)-ones catalyzed by cerium ammonium nitrate via Hantzsch multi-component reaction and their antibacterial activity. *Heterocycl. Chem.* **2016**, *52*, 409−414.
(33) Govindaraju, S.; Tabassum, S.; Khan, R. U. R.; Pasha, M. A. Catalyst-free green synthesis of novel 2-amino-4-aryl-3-(4-fluorophenyl)-4,6,7,8-tetrahydroquinolin- 5(1H)-ones via a one-pot four-component reaction under ultrasonic condition. *Heterocycl. Chemi.* **2016**, *52*, 964−969.
(34) Balasubramaniam, B.; Prateek Ranjan, S.; Ranjan, S.; Saraf, M.; Kar, P.; Singh, S. P.; Thakur, V. K.; Singh, A.; Gupta, R. K. Antibacterial and antiviral functional materials: chemistry and biological activity toward tackling COVID-19-like pandemics. *ACS Pharmacol. Transl. Sci.* **2020**, *4* (1), 8−54.
(35) Singh, K.; Mishra, A.; Sharma, D.; Singh, K. Antiviral and antimicrobial potentiality of nano drugs. In *Applications of Targeted Nano Drugs and Delivery Systems*; Elsevier, 2019; pp 343−356.
(36) Brandelli, A.; Lopes, N. A.; Boelter, J. F. Food applications of nanostructured antimicrobials. In *Food Preservation*; Academic Press, 2017; pp 35−74.
(37) Soyingbe, O. S.; Mongalo, N. I.; Makhafola, T. J. In vitro antibacterial and cytotoxic activity of leaf extracts of Centella asiatica (L.) Urb, Warburgia salutaris (Bertol. F.) Chiov and Curtisia dentata (Burm. F.) CA Sm-medicinal plants used in South Africa. *BMC Complementary Med. Ther.* **2018**, *18*, 315−410.
(38) Hawata, M. A.; El-Essawy, F.; El-Sayed, W. A.; El-Bayaa, M. Synthesis and Cytotoxic Activity of New Substituted Pyrazolo[3,4-b]pyridine Derivatives and Their Acyclic Nucleoside Analogs. *Egypt. J. Chem.* **2022**, *65* (3), 161−169.
(39) Elsherif, M. A. Antibacterial evaluation and molecular properties of pyrazolo[3,4-b] pyridines and thieno[2,3-b]pyridines. *J. Appl. Pharm. Sci.* **2021**, *11* (6), 118−124.
(40) El-Gohary, N. S.; Gabr, M. T.; Shaaban, M. I. Synthesis, molecular modeling and biological evaluation of new pyrazolo[3,4-b]pyridine analogs as potential antimicrobial, antiquorum-sensing and anticancer agents. *Bioorg. Chem.* **2019**, *89*, 102976.

https://doi.org/10.1021/acsomega.4c09524
ACS Omega 2025, 10, 1643−1656

(41) Fouda, A. M.; Abbas, H. A. S.; Ahmed, E. H.; Shati, A. A.; Alfaifi, M. Y.; Elbehairi, S. E. I. Synthesis, in vitro antimicrobial and cytotoxic activities of some new pyrazolo[1,5-a]pyrimidine derivatives. *Molecules* **2019**, *24* (6), 1080.
(42) Loganathan, V.; Ahamed, A.; Radhakrishnan, S.; Z Gaafar, A. R.; Gurusamy, R.; Akbar, I. Synthesis of anthraquinone-connected coumarin derivatives via grindstone method and their evaluation of antibacterial, antioxidant, tyrosinase inhibitory activities with molecular docking, and DFT calculation studies. *Heliyon* **2024**, *10* (3), 25168.
(43) Loganathan, V.; Ahamed, A.; Akbar, I.; Alarifi, S.; Raman, G. Antioxidant, antibacterial, and cytotoxic activities of Cimemoxin derivatives and their molecular docking studies. *J. King Saud Univ., Sci.* **2024**, *36* (1), 103011.
(44) Kumar, R. S.; Idhayadhulla, A.; Nasser, A.; Murali, K. Synthesis and anticancer activity of some new series of 1, 4-dihydropyridine derivatives. *Indian J. Chem., Sect. B:Org. Chem. Incl. Med. Chem.* **2011**, *50* (8), 1140−1144.
(45) Loganathan, V.; Akbar, I.; Ahmed, M. Z.; Kazmi, S.; Raman, G. Spectroscopic studies on the antioxidant and anti-tyrosinase activities of anthraquinone derivatives. *J. King Saud Univ., Sci.* **2023**, *35* (10), 102971.
(46) Mullaivendhan, J.; Akbar, I.; Gatasheh, M. K.; Hatamleh, A. A.; Ahamed, A.; Abuthakir, M. H. S.; Gurusamy, R. Cu(II)-catalyzed: synthesis of imidazole derivatives and evaluating their larvicidal, antimicrobial activities with DFT and molecular docking studies. *BMC Chem.* **2023**, *17* (1), 155.
(47) Loganathan, V.; Radhakrishnan, S.; Ahamed, A.; Gurusamy, R.; Abd-Elkader, O. H.; Idhayadhulla, A. Cu (II)-tyrosinase enzyme catalyst mediated synthesis of mosquito larvicidal active pyrazolidine-3, 5-dione derivatives with molecular docking studies and their ichthyotoxicity analysis. *Pone* **2024**, *19* (9), No. e0298232.
(48) Loganathan, V.; Akbar, I.; Ahamed, A.; Alodaini, H. A.; Hatamleh, A. A.; Abuthkir, M. H. S.; Gurusamy, R. Synthesis, antimicrobial and cytotoxic activities of tetrazole N-Mannich base derivatives: Investigation of DFT calculation, molecular docking, and Swiss ADME studies. *J. Mol. Struct.* **2024**, *1300*, 137239.
(49) Wang, G. W.; Miao, C. B. Environmentally benign one-pot multi-component approaches to the synthesis of novel unsymmetrical 4-arylacridinediones. *Green Chem.* **2006**, *8* (12), 1080−1085.
(50) To, Q. H.; Lee, Y. R.; Kim, S. H. Efficient synthesis of tetrahydroquinolinones by acetic acid-mediated formal[3 + 3]-cycloaddition. Monatsh. Chemie. *Chem. Month.* **2012**, *143*, 1421−1426.
(51) Vidali, V. P.; Nigianni, G.; Athanassopoulou, G. D.; Canko, A.; Mavroidi, B.; Matiadis, D.; Pelecanou, M.; Sagnou, M. Synthesis of Novel Pyrazolo[3,4-b]pyridines with Affinity for β-Amyloid Plaques. *Molbank* **2022**, *2022* (1), M1343.
(52) Santoro, A.; Tuyèras, F.; Dupeyre, G.; Laine, P. P.; Ciofini, I.; Nastasi, F.; Campagna, S. Pyrimidyl-substituted anthracene fluorophores: Syntheses, absorption spectra, and photophysical properties. *Dyes Pigm.* **2018**, *159*, 619−636.
(53) McGaw, L. J.; Elgorashi, E. E.; Eloff, J. N. Cytotoxicity of African medicinal plants against normal animal and human cells. In *Toxicological Survey of African Medicinal Plants*; Elsevier, 2014; pp 181−233.
(54) Agu, P. C.; Afiukwa, C. A.; Orji, O. U.; Ezeh, E. M.; Ofoke, I. H.; Ogbu, C. O.; Ugwuja, E. I.; Aja, P. M. Molecular docking as a tool for the discovery of molecular targets of nutraceuticals in diseases management. *Sci. Rep.* **2023**, *13* (1), 13398.
(55) Asiamah, I.; Obiri, S. A.; Tamekloe, W.; Armah, F. A.; Borquaye, L. S. Applications of molecular docking in natural products-based drug discovery. *Sci. Afr.* **2023**, *20*, No. e01593.
(56) Naithani, U.; Guleria, V. Integrative computational approaches for discovery and evaluation of lead compound for drug design. *Front. Drug Des. Discovery* **2024**, *4*, 1362456.
(57) Shaker, B.; Ahmad, S.; Lee, J.; Jung, C.; Na, D. In silico methods and tools for drug discovery. *Comput. Biol. Med.* **2021**, *137*, 104851.
(58) Berk, B.; Kaynar, G.; Erta, M.; Biltekin, S. N. Molecular modelling and compound activity of the Escherichia Coli and Staphylococcus Aureus DNA Gyrase B ATPase site. *Acta Pharm. Sin.* **2017**, *55* (1), 97−117.
(59) Sharma, S.; Tyagi, R.; Srivastava, M.; Rani, K.; Kumar, D.; Asthana, S.; Raj, V. S. Identification and validation of potent inhibitor of Escherichia coli DHFR from MMV pathogen box. *J. Biomol. Struct. Dyn.* **2022**, *41* (11), 1−10.
(60) Khodair, A. I.; Ahmed, A.; Imam, D. R.; Kheder, N. A.; Elmalki, F.; Hadda, T. B. Synthesis, antiviral, DFT and molecular docking studies of some novel 1,2,4-triazine nucleosides as potential bioactive compounds. *Carbohydr. Res.* **2021**, *500*, 108246.
(61) Rachedi, K. O.; Ouk, T. S.; Bahadi, R.; Bouzina, A.; Djouad, S. E.; Bechlem, K.; Zerrouki, R.; Ben Hadda, T.; Almalki, E.; Berredjem, M. Synthesis, DFT and POM analyses of cytotoxicity activity of α-amidophosphonates derivatives: Identification of potential antiviral O,O-pharmacophore site. *J. Mol. Struct.* **2019**, *1197*, 196−203.
(62) Qi, L.; Li, M. C.; Bai, J. C.; Ren, Y. H.; Ma, H. X. In vitro antifungal activities, molecular docking, and DFT studies of 4-amine-3-hydrazino-5-mercapto-1,2,4-triazole derivatives. *Bioorg. Med. Chem. Lett.* **2021**, *40*, 127902.
(63) Nural, Y.; Ozdemir, S.; Yalcin, M. S.; Demir, B.; Atabey, H.; Seferoglu, Z.; Ece, A. New bis-and tetrakis-1,2,3-triazole derivatives: Synthesis, DNA cleavage, molecular docking, antimicrobial, anti-oxidant activity and acid dissociation constants. *Bioorg. Med. Chem. Lett.* **2022**, *55*, 128453.
(64) Hassan, S. A.; Ziwar, J. B.; Aziz, D. m.; Abdullah, M. N. Sonochemical synthesis of New Thiazolidin-4-one derivatives as potent anticancer and antimicrobial agents with Docking design, and Energy gap estimation. *J. Mol. Struct.* **2024**, *1301*, 137282.
(65) Abdullah, M. N.; Osw, P.; Hassan, S. A.; Othman, S. Two new cyclohexenone derivatives: Synthesis, DFT estimation, biological activities and molecular docking study. *J. Mol. Struct.* **2024**, *1301*, 137361.
(66) Sliwoski, G.; Kothiwale, S.; Meiler, J.; Lowe, E. W. Computational methods in drug discovery. *Pharm. Rev.* **2014**, *66*, 334−395.
(67) Loganathan, V.; Mani, A.; Akbar, I.; Ahamed, A.; Alodaini, H. A.; Gerbu, D. G.; Manilal, A. Synthesis, antimicrobial, antioxidant, tyrosinase inhibitory activities, and computational studies of novel chromen[2,3-c]pyrazole derivatives. *Mol. Divers.* **2024**, 1−21.
(68) Ononamadu, C. J.; Ibrahim, A. Molecular docking and prediction of ADME/drug- likeness properties of potentially active antidiabetic compounds isolated from aqueous-methanol extracts of Gymnema sylvestre and Combretum micranthum. *Biotechnologia* **2021**, *102* (1), 85.
(69) Macabeo, A. P. G.; Pilapil, L. A. E.; Garcia, K. Y. M.; Quimque, M. T. J.; Phukhamsakda, C.; Cruz, A. J. C.; Hyde, K. D.; Stadler, M. Alpha-glucosidase-and lipase- inhibitory phenalenones from a new species of Pseudolophiostoma originating from Thailand. *Molecules* **2020**, *25* (4), 965.
(70) Aliye, M.; Dekebo, A.; Tesso, H.; Abdo, T.; Eswaramoorthy, R.; Melaku, Y. Molecular docking analysis and evaluation of the antibacterial and antioxidant activities of the constituents of Ocimum cufodontii. *Sci. Rep.* **2021**, *11* (1), 10101.
(71) Jorepalli, S.; Adikay, S.; Chinthaparthi, R. R.; Gangireddy, C. S. R.; Koduru, J. R.; Karri, R. R. Synthesis, molecular docking studies and biological evaluation of N-(4- oxo-2-(trifluoromethyl)-4H-chromen-7-yl)benzamides as potential antioxidant, and anticancer agents. *Sci. Rep.* **2024**, *14* (1), 9866.
(72) Sun, Y.; Wang, L.; Sun, Y.; Wang, J.; Xue, Y.; Wu, T.; Yin, W.; Qin, Q.; Sun, Y.; Wang, H.; et al. Structure-based discovery of 1-(3-fluoro-5-(5-(3-(methylsulfonyl)phenyl)-1H-pyrazolo[3,4-b] pyridin-3-yl) phenyl)-3-(pyrimidin-5-yl) urea as a potent and selective nanomolar type-II PLK4 inhibitor. *Eur. J. Med. Chem.* **2022**, *243*, 114714.
(73) Sun, Y.; Tang, H.; Wang, X.; Feng, F.; Fan, T.; Zhao, D.; Xiong, B.; Xie, H.; Liu, T. Identification of 1H- pyrazolo[3,4-b]pyridine derivatives as novel and potent TBK1 inhibitors: design, synthesis,

https://doi.org/10.1021/acsomega.4c09524
ACS Omega 2025, 10, 1643−1656

biological evaluation, and molecular docking study. *J. Enzyme Inhib. Med. Chem.* **2022**, *37* (1), 1411−1425.

https://doi.org/10.1021/acsomega.4c09524
ACS Omega 2025, 10, 1643−1656